Chinese Chemical Letters 32 (2021) 4058–4062

Contents lists available at ScienceDirect

Chinese Chemical Letters

journal homepage: www.elsevier.com/locate/cclet

Communication

Alopecuroidines A–C, three matrine-derived alkaloids from the seeds of *Sophora alopecuroides*

Xiang Yuan, Zhenyuan Li, Ziming Feng, Jianshuang Jiang, Yanan Yang, Peicheng Zhang*

State Key Laboratory of Bioactive Substance and Function of Natural Medicines, Institute of Materia Medica, Chinese Academy of Medical Sciences and Peking Union Medical College, Beijing 100050, China

ARTICLE INFO

Article history:
Received 4 February 2021
Revised 5 April 2021
Accepted 12 April 2021
Available online 23 April 2021

Keywords:
Alkaloids
Sophora alopecuroides
X-ray diffraction
Anti-proliferative
Apoptosis

ABSTRACT

Three matrine-derived alkaloids, alopecuroidine A (**1**), alopecuroidine B (**2a**) and alopecuroidine C (**2b**) were isolated from the seeds of *Sophora alopecuroides*. Their structures were elucidated by extensive spectroscopic analyses and X-ray diffraction. Three compounds possess an unprecedented rearranged fused 7/6/5/6 tetracyclic skeleton with a diazacycloheptane structure. Their plausible biosynthetic pathway was also proposed. The anti-proliferative activities of compounds **1** and **2a** were examined by the MTT assay. Compound **1** inhibited the viability of human lung cancer A549 cells, having a half maximal inhibitory concentration (IC_{50}) of 7.58 ± 2.47 μmol/L at 72 h. The flow cytometric analysis suggested that **1** inhibited A549 cell growth by inducing apoptosis and cell-cycle arrest. Additionally, **1** induced the loss of mitochondrial membrane potential, elevated intracellular reactive oxygen species, increased the Bax/Bcl-2 ratio, stimulated cleaved-caspase-3 and P53 protein levels, and suppressed the pro-caspase-3 level. Thus, **1** appeared to induce A549 cells apoptosis through a mitochondria-mediated apoptotic pathway.

Quinolizidine alkaloids are one kind of characteristic metabolite from the genus *Sophora* (Leguminosae), which include matrine-type, sparteine-type, cytisine-type and aloperine-type alkaloids. Based on their structural diversities and pharmacological significance, these alkaloids, especially matrine-type alkaloids, have continuously elicited considerable interest from both natural product and synthetic chemists over the past several decades [1–5]. "Ku Dou Zi" [*Sophora alopecuroides* L. (*S. alopecuroides*)], belonging to the *Sophora* genus, is a perennial plant that grows on desolate salt marshes, or saline-alkali lands and is mainly distributed in China's northwest desert region [6,7]. The seeds of this plant have a long history in traditional Chinese medicine for the treatment of eczema, acute pharyngolaryngeal infection, sore throat, acute dysentery and gastrointestinal hemorrhage [8–11]. Studies have shown that matrine-type alkaloids are the principal bioactive components in *S. alopecuroides* and display a variety of important biological activities, including potential sedative, analgesic, antiviral, antitumor, anti-fibrosis, anti-inflammatory and antibacterial activities [12–15]. Some matrine-type compounds, especially sophoridine and matrine, possess excellent anti-carcinogenic activities [16].

Matrine-type alkaloids contain 15 basic carbon atoms with a 6/6/6/6 tetracyclic skeleton. In recent years, many matrine-based compounds have been isolated from the *Sophora* genus, such as rearranged 6/6/6/4 or 6/5/6/6 tetracyclic skeletons, 10/6/6 tricyclic skeleton with cleavage of the C-5–C-6 bond, matrine-type alkaloids with an open-loop D ring, and a series of dimers connected by carbon-carbon single bonds [1,3,6,12,17]. In our study, the water extract of the seeds of *S. alopecuroides* was investigated, leading to the isolation and characterization of three compounds that possess an unprecedented rearranged fused 7/6/5/6 tetracyclic skeleton with a diazacycloheptane structure, namely alopecuroidine A (**1**), alopecuroidine B (**2a**) and alopecuroidine C (**2b**). Here, compounds **1** and **2a** were evaluated for their anti-proliferative effects on human lung cancer A549 cells. The results indicated that **1** inhibited the proliferation of A549 cells by arresting the cell cycle in the G1 phase and induced the apoptosis of A549 cells through the mitochondrial pathway.

Compound **1** was assigned its molecular formula of $C_{15}H_{20}N_2O_2$ by the HRESIMS ion at *m/z* 261.1596 $[M + H]^+$, requiring the presence of seven degrees of unsaturation. Its infrared spectroscopy (IR) spectrum showed the existence of an amido carbonyl group (1620 cm^{-1}).

The ^1H nuclear magnetic resonance (NMR) spectrum (Table 1) of **1** showed two characteristic methylenes at δ_H 3.56 (1H, dd, J = 14.0, 7.0 Hz, H-2b), 3.39 (1H, m, H-2a), 3.34 (1H, m, H-11a) and

* Corresponding author.
E-mail address: pczhang@imm.ac.cn (P. Zhang).

https://doi.org/10.1016/j.cclet.2021.04.022
1001-8417/

Table 1
^{1}H and ^{13}C NMR data for **1** and **2** in methanol-d_4 (δ in ppm, J in Hz).[a]

No.	**1**		**2**	
	δ_H	δ_C	δ_H	δ_C
2a	3.39, m	57.2	3.35, m	57.0
2b	3.56, dd, 14.0, 7.0		3.58, m	
3a	1.75, m	20.7	1.93, m	21.6
3b	1.98, m		2.34, m	
4a	2.68, m	41.8	2.73, m	42.1
4b	2.57, m		2.59, m	
5		191.6		193.8
6		113.4		113.7
7		157.9		156.3
8	2.64, m	51.4		77.3
9a	1.32, td, 13.0, 3.5	23.8	1.57, td, 13.0, 3.5	30.1
9b	2.07, m		1.99, m	
10a	2.27, m	21.4	2.24, m	19.3
10b	1.92, m		1.84, m	
11a	3.34, m	53.2	3.34, m	52.9
11b	3.28, td, 12.5, 5.0		3.27, td, 12.5, 5.0	
12	3.49, td, 11.0, 5.0	66.5	3.53, td, 11.0, 5.0	69.6
13a	2.23, m	28.2	2.05, m	21.2
13b	1.48, m		1.76, m	
14a	2.01, m	23.1	1.99, m	20.3
14b	1.83, m		1.81, m	
15a	2.20, m	33.3	2.21, m	33.2
15b	2.53, m		2.52, m	
16		168.8		170.1

[a] Overlapped signals are reported without designating multiplicity.

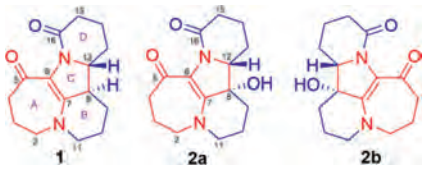

Fig. 1. Chemical structures of compounds **1**, **2a** and **2b**.

3.28 (1H, td, J = 12.5, 5.0 Hz, H-11b), and a methine at 3.49 (1H, td, J = 11.0, 5.0 Hz, H-12). Analysis of the ^{13}C NMR and HSQC data indicated 15 carbons, which were assigned as two carbonyl carbons (δ_C 191.6, 168.8), two double bond carbons (δ_C 157.9, 113.4), two methine carbons (δ_C 66.5, 51.4), and nine methylene carbons (two of which were connected to heteroatoms at δ_C 57.2 and 53.2). The carbonyls and double bond were assigned as three of the seven degrees of unsaturation, demonstrating the presence of a tetracyclic ring system in **1** (Fig. 1).

Assembly of the structure of **1** was accomplished mainly by using the results of 2D NMR experiments. The $^{1}H-^{1}H$ COSY correlations of H_2-2/H_2-3/H_2-4 and H_2-11/H_2-10/H_2-9/H-8/H-12/H_2-13/H_2-14/H_2-15 displayed the presence of two isolated spin systems. The HMBC spectrum (Fig. 2) demonstrated the long-range correlations of H-12, H_2-14 and H_2-15 with the carbonyl carbon C-16, which confirmed the presence of a δ-lactam. In addition, correlations from H_2-4 to C-2, C-3, C-5 and C-6, from H-8 to C-7, C-9 and C-13, and from H-12 to C-8, C-9 and C-13 indicated the presence of an unsaturated ketone system at C-5 (δ_C 191.6), a double bond located between C-6 and C-7. Meanwhile, the HMBC correlations from H_2-2 to C-3, C-4 and C-7, from H_2-11 to C-7, C-9 and C-10 combined with the $^{1}H-^{1}H$ COSY correlations suggested that ring A was a seven-membered ring and ring B was a six-membered ring. Therefore, the planar structure of **1** possessing an unprecedented carbon skeleton comprising a fused 7/6/5/6 rearranged tetracyclic was determined.

The ROESY data were utilized to assign the relative configurations in **1**. The ROESY spectrum revealed the correlations of H-8/H-13b, H-8/H-9b and H-12/H-13a indicating that H-8 and H-12 might possess different orientations in **1**. Supporting the assignment were the calculated ^{13}C NMR chemical shifts for two diastereomers, 8*R**,12*R**-**1** and 8*S**,12*R**-**1**, of which the 8*R**,12*R**-**1** matched well with the NMR experimental data with a high probability of 100% (Supporting information). Furthermore, the possible configurations of **1** were established by comparing the experimental electronic circular dichroism (ECD) spectrum with the calculated ECD spectra of the B3LYP/6–311+G(d,p) optimized conformer acquired by the quantum chemical time dependent density functional theory (TDDFT) calculation (see supporting information). The experimental ECD curve of **1** correlated well with that calculated for (8*R*,12*R*)-**1** in the range of 200 nm to 400 nm (Fig. 2). Furthermore, we showed that **1** was optically pure by chiral-phase HPLC using CHIRALPAK AD-H and AD-RH columns. Therefore, the structure of compound **1** was determined and named alopecuroidine A.

Compound **2** was assigned its molecular formula of $C_{15}H_{20}N_2O_3$ by the HRESIMS ion at m/z 277.1546 $[M + H]^+$, requiring the presence of seven degrees of unsaturation. Its IR spectrum exhibited absorption peaks corresponding to hydroxyl (3279 cm^{-1}) and amide carbonyl group (1642 cm^{-1}).

Detailed analyses of the molecular weight and NMR data suggested that **2** was very similar to **1**, but **2** should have one more oxygen than **1**. The only difference was that a methine carbon at C-8 (δ_C 51.4) in that of **1** was replaced by an oxygenated quaternary carbon (δ_C 77.3) at the same position in **2**. This speculation was further supported by the $^{1}H-^{1}H$ COSY correlations of H_2-2/H_2-3/H_2-4, H_2-11/H_2-10/H_2-9 and H-12/H_2-13/H_2-14/H_2-15, three spin systems, together with the HMBC correlations between H_2-9 and C-7 (δ_C 156.3), C-8 (δ_C 77.3) and C-12 (δ_C 69.6), between H-12 and C-8, and between H_2-13 and C-8 and C-12 (Fig. 2). This assumption was further proven by the change in the chemical shifts of C-7, C-9, C-12 and C-13 from δ_C 157.9, 23.8, 66.5 and 28.2 in **1** to δ_C 156.3, 30.1, 69.6 and 21.2 in **2**, respectively. Accordingly, the planar structure of **2** was determined as shown in Fig. 1.

To determine the absolute configuration, **2** was cultured as single crystal. The X-ray diffraction of single crystal results indicated that the single crystal from **2** was a pair of enantiomers. The combined optical rotation data (the rotation value is not zero) suggested that **2** is not an equal pair of enantiomers. For confirming this fact, the chiral-column HPLC analysis of **2** was performed and showed two peaks with peak area ratio of 95:5. The compound **2** were separated by chiral-phase HPLC to obtain two compounds **2a** and **2b** (Fig. 1). Fortunately, the single crystal of **2a** suitable for X-ray diffraction were obtained [Cu Kα radiation, Flack parameter 0.01 (16)]. The absolute configuration of **2a** was determined to be 8*S*,12*R* and the absolute configuration of compound **2b** was subsequently confirmed by comparing the experimental and calculated ECD spectra and determined to be 8*R*,12*S* (Fig. 2). Therefore, the structures of **2a** and **2b** were determined and named as alopecuroidine B and alopecuroidine C, respectively.

A plausible biogenetic pathway for isolated compounds is presented in Scheme 1. Biosynthetically, these compounds might originate from a matrine-type precursor, sophoridine, a typical abundant component in the *Sophora* genus [18]. Firstly, sophoridine undergoes a dehydration reaction to produce intermediate I. Intermediate I is subsequently involved an oxidative cleavage of the double bond to generate intermediate II, followed by an aldol reaction to obtain intermediate III. Intermediate III is converted to compound **1** through a dehydration reaction. **1** is converted to IV through an aromatization reaction. Intermediate IV is converted to **2a** and **2b** through hydration reaction. To the best of our knowledge, the C-11 configuration of matrine-type alkaloids from natural resource has all been in the *R* configuration. Interestingly, **2b** is the first natural matrine-type alkaloid isolated from *Sophora* plants possessing a 12*S* configuration (matrine was located at C-11).

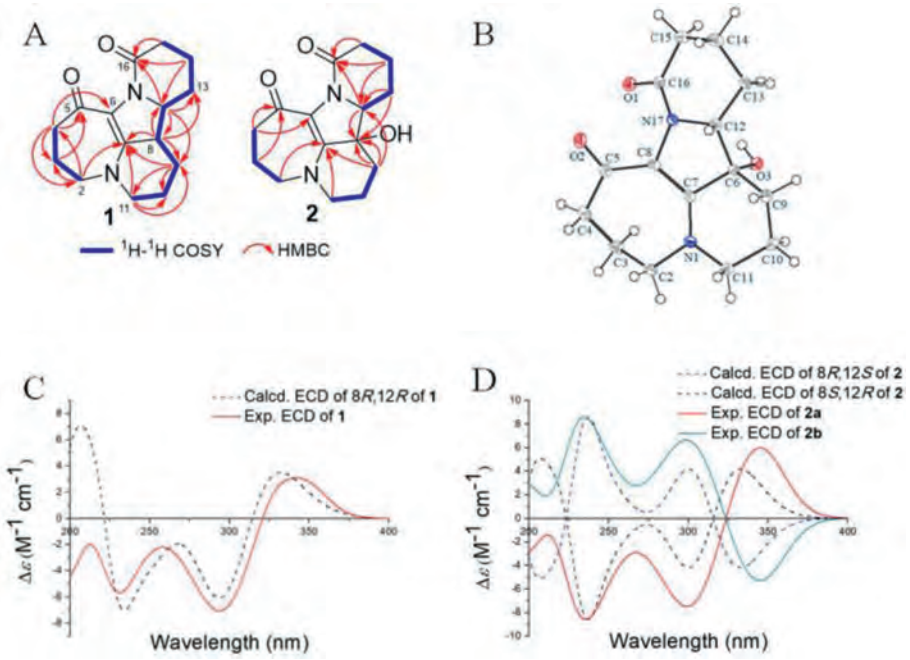

Fig. 2. ^{1}H−^{1}H COZY and HMBC correlations of **1** and **2** (A). Single crystal X-ray structure of **2a** (B). Calculated and experimental ECD spectra of **1** (C), **2a** and **2b** (D).

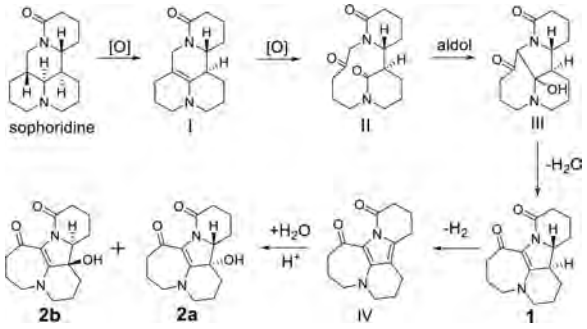

Scheme 1. Hypothetical biosynthetic pathways for **1**, **2a** and **2b**.

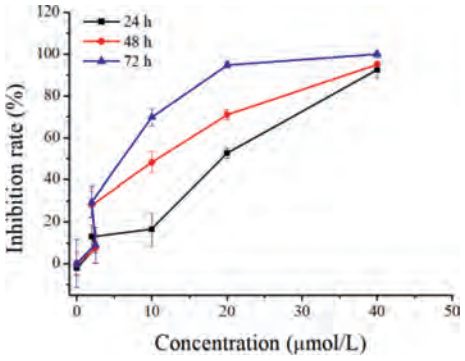

Fig. 3. Inhibition rates of **1** on the proliferation of A549 cells. A549 cells were seeded onto 96-well plates and incubated for 24, 48 or 72 h with increasing concentrations (0–40 μmol/L) of 1, and cell viability was examined using the MTT method. The data are presented as mean ± SD of triplicates experiments.

Compounds **1** and **2a** (0−40 μmol/L) were tested for their anti-proliferative activities against A549 cells at 24 h. Compound **1** exhibited a potent anti-proliferative effect against A549 cells, resulting in a half maximal inhibitory concentration (IC_{50}) value of 20.92 ± 3.03 μmol/L, whereas **2a** had values greater than 40 μmol/L. Subsequently, we tested the anti-proliferative effect of **1** on A549 cells at 48 and 72 h (Fig. 3), and the IC_{50} values were 12.82 ± 1.39 μmol/L and 7.58 ± 2.47 μmol/L, respectively. Therefore, we used 5, 10 or 15 μmol/L of **1** to conduct the subsequent experiments.

To further study the correlation between the anti-proliferative effect and both cell cycle arrest and apoptosis, the A549 cells were treated with **1** (5, 10 and 15 μmol/L) for 24 h. Flow cytometry assays were performed to quantify the cell apoptotic rates using Annexin VFITC/PI double staining. As shown in Fig. 4, **1**-treated A549 cells had increased percentages of early and late apoptotic cells in a dose-dependent manner. Approximately 6.38% of apoptotic cells were observed in the control group, while they increased to 7.02%, 8.56% and 30.41% after treatment with 5, 10 and 15 μmol/L of **1** for 24 h, respectively, indicating that **1** effectively promoted the apoptosis of A549 cells (Fig. 4).

Cell cycle arrest is considered a critical control point for the management of cancer cell growth. As shown in Fig. 4, treated cells accumulated in the G1 phase. The proportions of cells in the G1 phase were 50.40%, 45.10%, 72.56% and 75.94% in the 0, 5, 10 and 15 μmol/L **1**-treatment groups, respectively. The results indicated that **1** blocked the cell cycle at the G1 phase, resulting in apoptosis (Fig. 4).

Mitochondria play important roles in drug-induced apoptosis [19]. Therefore, we examined the correlation between **1**-induced apoptosis and mitochondrial membrane potential ($\Delta\psi$m) in A549 cells. As shown in Fig. S1 (Supporting information), treatment with increasing **1**′s concentrations induced a loss of $\Delta\psi$m in a dose-dependent manner. Additionally, the overproduction of reactive oxygen species (ROS) may be a consequence of mitochondrial dysfunction, which is a typical characteristic of intrinsic apoptosis. Therefore, the intracellular ROS levels in A549 cells were also determined by 5(6)-carboxy-2′,7′-dichlorofluorescein diacetate (DCFH-DA) staining. As shown in Fig. S1, compared with the control group, the intracellular ROS levels clearly increased in A549 cells after treatment with **1**. Thus, **1** caused mitochondrial dysfunction in A549 cells, resulting in increased intracellular ROS levels and decreased mitochondrial $\Delta\psi$m values (Supporting information).

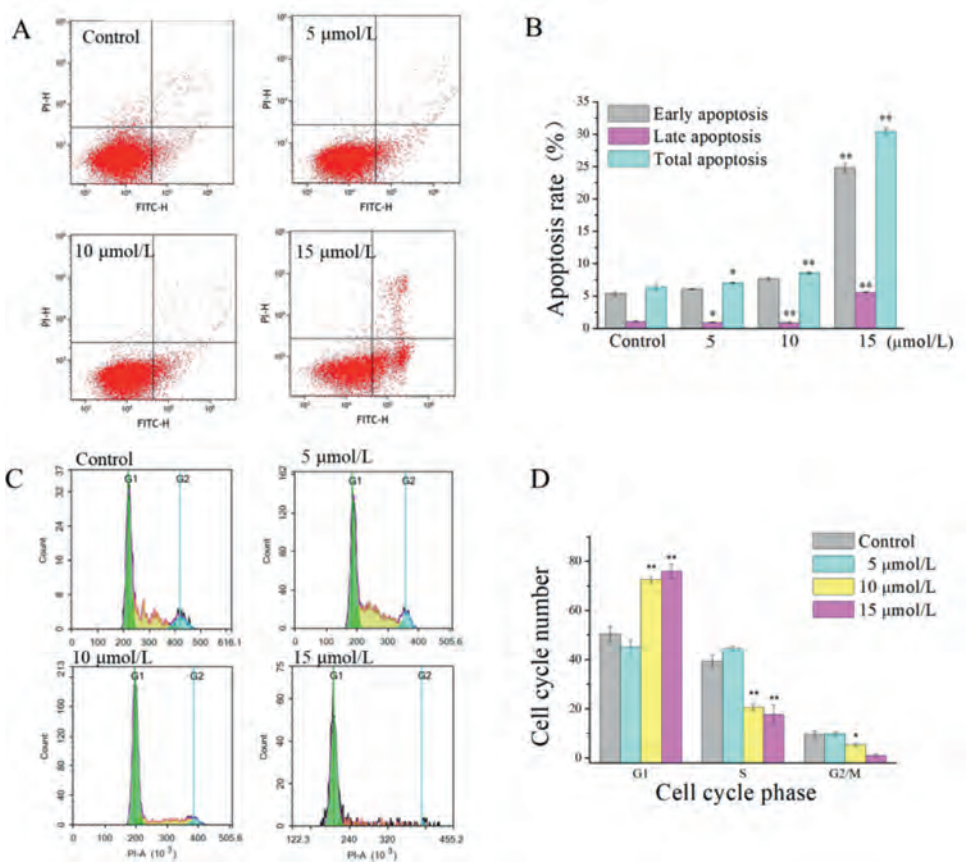

Fig. 4. Flow cytometric analysis of the cell cycle arrest and apoptotic effects induced by **1** (0, 5, 10 and 15 μmol/L) in A549 cells. (A) Apoptotic rates were assessed using Annexin-V/PI double staining. (B) Quantitative analysis of the numbers of apoptotic cells. (C) The effects of **1** on cell cycle were analyzed by flow cytometry. (D) Relative percentages of cells in the G1, S and G2/M phages. Data are shown by mean ± SD ($n = 3$). * $P < 0.05$, ** $P < 0.01$ *vs.* control.

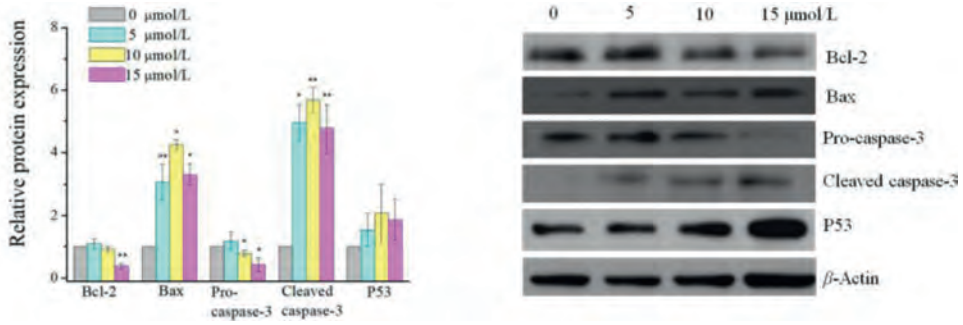

Fig. 5. Effects of **1** on the apoptosis-associated protein levels in A549 cells. The A549 cells were treated with **1** (0, 5, 10 and 15 μmol/L) for 24 h. The cells were performed on Western blot analysis as described in Supporting information. Bax, Bcl-2, pro-caspase-3, cleaved caspase-3 and P53 protein expressions were shown. β-Actin was employed as an internal control. Data are shown by mean ± SD ($n = 2$–3). * $P < 0.05$, **$P < 0.01$ *vs.* control.

To confirm the molecular mechanism underlying **1**-induced apoptosis in A549 cells, the expression of mitochondria-mediated apoptotic pathway proteins were examined by western blotting. As shown in Fig. 5, **1** dose-dependently increased the expression of the pro-apoptotic protein Bax but decreased the expression of the anti-apoptotic protein Bcl-2 in A549 cells. Furthermore, **1** significantly upregulated the expression levels of cleaved caspase-3 and P53, but downregulated that of pro-caspase-3, indicating its involvement in the mitochondrial pathway (Fig. 5).

In conclusion, three novel skeleton alkaloids were isolated from the seeds of *S. alopecuroides*. They represent the first examples of matrine-based alkaloids with a 7/6/5/6 ring framework. The most intriguing feature is the unusual diazacyclohepta[jk]fluorene-7,8(4*H*)-dione moiety, which is very rare in natural products. Interestingly, compound **2** is a pair of unequal enantiomers with a ratio of 95:5. The corresponding optically pure compound was successfully separated by chiral-column HPLC, and the absolute configuration was determined by X-ray diffraction. We also examined the anticancer activities of compounds **1** and **2a** on A549 cells *in vitro*. Compound **1** significantly inhibited the proliferation of A549 cells, with an IC_{50} of 7.58 ± 2.47 μmol/L at 72 h, and it induced cell cycle arrest in the G1 phase in a dose-dependent manner. Furthermore, **1** induced A549-cell apoptosis through a mitochondria-mediated intrinsic apoptotic pathway, which included the dissipation of $\Delta\psi$m, overproduction of intracellular ROS, dysregulation of Bax/Bcl-2, and activation of cleaved

caspase-3 and P53. Our findings indicated that **1** might be a potential candidate for the treatment of lung cancer.

Declaration of competing interest

The authors declare no competing financial interest.

Acknowledgments

This work was supported by grants from CAMS Innovation Fund for Medical Sciences (No. 2016-I2M-1-010, China) and the Drug Innovation Major Project (No. 2018ZX09711001-008, China).

Appendix A. Supplementary data

Supplementary material associated with this article can be found, in the online version, at doi:10.1016/j.cclet.2021.04.022.

References

[1] Y.B. Zhang, L. Yang, D. Luo, et al., Org. Lett. 20 (2018) 5942–5946.
[2] A.D. Brosius, L.E. Overman, L. Schwink, J. Am. Chem. Soc. 121 (1999) 700–709.
[3] Y.B. Zhang, X.L. Zhang, N.H. Chen, et al., Org. Lett. 19 (2017) 424–427.
[4] A.D. Brosius, L.E. Overman, J. Org. Chem. 62 (1997) 440–441.
[5] X.R. He, J.C. Fang, L.H. Huang, et al., J. Ethnopharmacal. 172 (2015) 10–29.
[6] H.Y. Gao, G.Y. Li, J.H. Wang, Helv. Chim. Acta 95 (2012) 1108–1113.
[7] M.K. Panthati, K. Rao, S. Sandhya, et al., Rev. Bras. Farmacogn. 22 (2012) 1145–1154.
[8] K. Saito, N. Arai, T. Sekine, et al., Planta Med. 56 (1990) 487–488.
[9] P. Xiao, J. Li, H. Kubo, et al., J. Nat. Prod. 63 (2000) 190–192.
[10] J. Kwon, S. Basnet, J.W. Lee, et al., Med. Chem. Lett. 25 (2015) 3314–3318.
[11] Y.B. Zhang, L.Q. Zhan, G.Q. Li, et al., J. Org. Chem. 81 (2016) 6273–6280.
[12] Q.M. Pan, Y.H. Li, J. Hua, et al., J. Nat. Prod. 78 (2015) 1683–1688.
[13] L.Q. Li, X.L. Li, L. Wang, et al., Cell. Physiol. Biochem. 30 (2012) 631–641.
[14] J.R. Guzman, J.S. Koo, J.R. Goldsmith, et al., Sci. Rep. 3 (2013) 1629.
[15] Y. Li, G. Wang, J. Liu, et al., Eur. J. Med. Chem. 188 (2020) 111972.
[16] Y.B. Zhang, D. Luo, L. Yang, et al., J. Nat. Prod. 81 (2018) 2259–2265.
[17] L. Wang, X.D. Wu, J. He, et al., Chem. Nat. Comp. 50 (2014) 876–879.
[18] M. Abatea, A. Festa, M. Falco, et al., Semin. Cell Dev. Biol. 98 (2020) 139–153.